AIAA JOURNAL
Vol. 30, No. 2, February 1992

Shape-Sensitivity Analysis and Design Optimization of Linear, Thermoelastic Solids

Gene J. W. Hou,* Jeen S. Sheen,† and Ching H. Chuang†
Old Dominion University, Norfolk, Virginia 23529

In this study, a numerical scheme is developed for shape-sensitivity analysis and design optimization of linear, quasistatic, thermoelastic solids. In this scheme, the finite-element method is used as the analyzer for analyzing stress, temperature, shape sensitivity, and design velocity field. Based upon the method of material derivatives, both the techniques of the direct-differentiation method and the adjoint-variable method are applied to derive the shape-sensitivity equations. The shape-optimization formulations discussed here include boundary integrals of displacements and heat fluxes as well as domain integrals of stresses and areas. Numerical results show that the proposed scheme works well in terms of accuracy.

Nomenclature

A_o = maximum allowable area
B_i = body force
b_i = design variable
C, D = $C = [C_{ijkl}]$ and $D = [D_{ijkl}]$, where C_{ijkl} and D_{ijkl} are material constants
F_b = objective function of the fixed-fixed beam problem
F_f = objective function of the thermal fin problem
f, β, γ = functions defined in the generic functional φ, i.e., $\varphi = \int_\Omega f \, d\Omega + \int_{\Gamma_a} \beta \, d\Gamma + \int_{\Gamma_b} \gamma \, d\Gamma$
g_1, g_2 = constraint functions
h = heat-convection coefficient
I = identity matrix
k = thermal conductivity
l_i = length of a line segment
P_0 = distributed load
Q = internal heat source
q = heat flux defined as $-k(\partial T/\partial n)$
T = temperature distribution
T_o = prescribed surface temperature
T_∞ = ambient temperature
t = surface tractions
t^o = prescribed surface tractions
$u(x)$ = displacement vector
$v(x)$ = velocity field vector
w = y-direction displacement
x = unperturbed position vector
x^* = perturbed position vector
y_o, y = initial and required y position of the upper boundary of the fixed-fixed beam
α = the coefficient of thermal expansion
Γ, Γ_i = unperturbed boundaries
ϵ, ϵ_{ij} = strain tensor
λ, ν = Lame's constants
σ, σ_{ij} = stress tensor
σ_o = Von Mises stress
σ_a = maximum allowable stress
τ = parameter monitoring domain variation
Ω = unperturbed configuration
Ω_e = domain of an element
Ω^* = perturbed configuration

Presented as Paper 90-1012 at the AIAA/ASME/ASCE/AHS/ASC 31st Structures, Structural Dynamics, and Materials Conference, Long Beach, CA, April 2–4, 1990; received July 26, 1990; revision received Dec. 13, 1990; accepted for publication Dec. 26, 1990.

*Associate Professor, Department of Mechanical Engineering and Mechanics. Member AIAA.
†Graduate Research Assistant, Deparment of Mechanical Engineering and Mechanics.

I. Introduction

APPLICATIONS of various computational methods to optimally design the shapes of elastic components have been the subject of study for more than two decades and have been documented in the literature.[1-5] The currently used approaches for shape-sensitivity analysis may be grouped into two main categories: the continuum approach and the discrete approach.

The continuum approach can be further classified into three groups according to the way the shape variations are defined: 1) method of material derivatives[4-6]; 2) generalized calculus of variations[7,8]; and 3) perturbation techniques.[9,10]

Although they employ different notations, all three methods yield a similar definition for shape variations. In this study, the method of material derivatives will be used for its simplicity in derivation.

In the discrete approach, the finite element method is commonly used to formulate the state equation in matrix form. The shape-sensitivity equations can then be obtained either by differentiating the matrix equations with respect to the design parmeters[11] or by using the finite difference method.[4] In this approach, the design parameters are the nodal coordinates of the finite element mesh.

As mentioned earlier, the method of material derivatives will be used in this study to investigate numerical schemes for shape-sensitivity analysis and design optimization. The concept of material derivatives is very similar to that of generalized calculus of variations.[2] Using the concept of material derivatives, methods for formulation and calculation of shape sensitivities can be further classified as the boundary method and the domain method, depending upon the form of the resulting sensitivity integrals.

The shape-sensitivity equation derived by the boundary method is usually represented by a boundary integral that is a functional of the partial shape derivatives of state variables. The domain method, on the other hand, yields a domain integral as the shape-sensitivity equation, which includes the total shape derivatives of state variables.

To evaluate the sensitivity equations derived by the boundary method, only the design velocity along the varied boundary must be specified. This is a considerable saving in computation. Nevertheless, the boundary method does not always yield accurate sensitivity information, particularly when the derived sensitivity equation is evaluated by the finite element method. As for the domain method, it is expensive in computation due to extra efforts needed to compute the domain design velocity. However, it can be comfortably used in conjunction with the finite element method. In fact, with a careful choice of the design velocity field, it has been proven that for some particular engineering applications the domain method is indeed equivalent to the discrete method.[13,14]

The main thrust of this research is to develop a reliable, finite-element-based scheme for shape-sensitivity analysis and optimization of linear, thermoelastic solids. Research efforts in this regard have been reported in the literature.[15,16] However, their efforts focused on theoretical derivation using the boundary method, whereas in this study, the domain method will be employed to derive sensitivity equations that will be evaluated by the finite element method. Furthermore, numerical studies will be conducted to investigate the performance of the developed finite-element-based scheme for sensitivity analysis as well as for design optimization. As mentioned previously, the reasons for selecting the finite element method to support computation are its accuracy and its convenience with regard to the sensitivity equations derived by the domain method. One particular development in this study is to circumvent numerical difficulties associated with boundary integrals that have not been effectively dealt with in many numerical shape-optimization schemes. The boundary integrals referred to here may be obtained from the mixed boundary conditions of the heat-transfer problem, which is a part of thermoelasticity, or may appear as constraints in terms of heat flux or displacement defined along the boundary.

In Sec. II, the problem statements and state equations regarding the shape optimal design of linear, quasistatic, thermoelastic solids are given. In Sec. III, both the direct-differentiation technique and the adjoint-variable technique will be employed in conjunction with the domain method to derive shape sensitivities of the functionals defined in Sec. II. In Sec. IV, a design procedure incorporated with the derived sensitivity equations for shape optimization of thermoelastic solids is presented. Numerical examples and their results are also included in this section to assess the performance of the proposed finite elemnt scheme. Finally, Sec. V outlines concluding remarks about this study.

II. Shape-Optimization Problems of a Thermal Fin and a Fixed-Fixed Beam

Examples of shape optimization of a thermal fin and a fixed-fixed beam will be defined in this section. These examples will serve as a vehicle to facilitate discussion on the shape-design sensitivity analysis and optimization of thermoelastic solids.

A. Optimal Design Problem Formulation

The purpose of a thermal fin is to dissipate heat in the solid to which it is attached. The heat flux goes through the base of a thermal fin whose cross section is shown in Fig. 1. In some applications, the thermal fin will constantly be operated under thermal stresses and deformations due to the rising temperature.

Let Ω, Γ, and x denote the undeformed domain, boundary, and coordinates, respectively. The objective of designing a thermal fin is to decide the best profile of the thermal fin such that the maximum amount of heat can be removed from the system, subject to area and stress constraints. Thus, the objective function can be stated as the total heat flux passing through the base of the fin. More specifically, the mathematical formulation of the aforementioned design optimization problem may be expressed as

$$\max_{\Gamma_2} F_f = \int_{\Gamma_1} q \, ds \tag{1}$$

$$g_1 = \int_\Omega d\Omega - A_o \leq 0 \tag{2}$$

$$g_2 = \int_\Omega (\sigma_o^2/\sigma_a^2 - 1) \, d\Omega \leq 0 \tag{3}$$

The functionals g_1 and g_2 defined in Eqs. (2) and (3) are associated with the area and the elemental stress constraints, respectively.

The second example will determine the initial geometry of a loaded, fixed-fixed beam shown in Fig. 2, subjected to an area constraint and a stress constraint, such that the top edge of the deformed beam will stay straight. The beam is subjected not only to a uniform load on Γ_3, but also various thermal boundary conditions that induce thermal deformations as well as stresses. These boundary conditions are stated as a heat-convection condition on Γ_4, a prescribed temperature condition on Γ_3, and a thermal insulation condition on Γ_5. Consequently, the beam can be modeled as a two-dimensional, thermoelastic solid. Note that the same notations are used here to denote the boundary contours of the thermal fin as well as

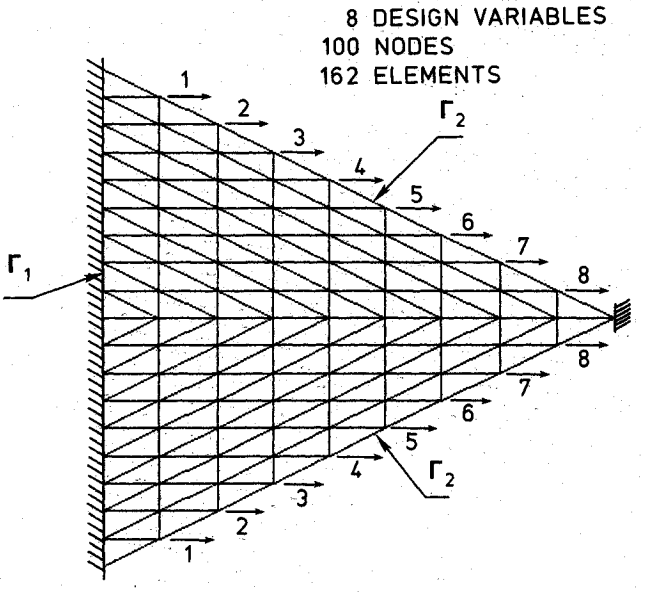

Fig. 1 Thermoelastic thermal fin.

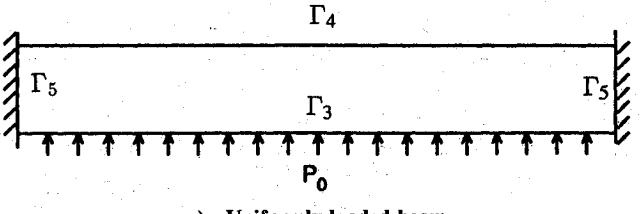

a) Uniformly loaded beam

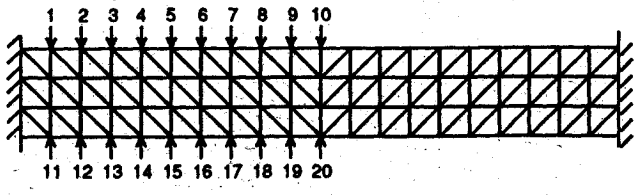

b) Numbering the design variables

Fig. 2 Fixed-fixed beam.

the fixed-fixed beam. Nevertheless, it should be understood that the entire boundary Γ of the domain Ω is equal to $\Gamma_1 \cup \Gamma_2$ for the thermal fin and equal to $\Gamma_3 \cup \Gamma_4 \cup \Gamma_5$ for the fixed-fixed beam.

The objective function of interest in a fixed-fixed beam may be stated as the deviation between the positions of the deformed boundary and the desired straight boundary. Choosing the x axis parallel to the beam axis, the objective function may be expressed as

$$F_b = \int_{\Gamma_4} (y + w - y_o)^2 \, ds$$

where the coordinates y and y_o specify the initial and the required positions of the boundary Γ_4, respectively, and $w(x)$ is the y direction displacement of point x on Γ_4. With an area and a stress constraint, the shape-optimization problem of concern can be mathematically defined as

$$\min_{\Gamma_3 \cup \Gamma_4} F_b = \int_{\Gamma_4} (y + w - y_o)^2 \, ds \tag{4}$$

subject to Eqs. (2) and (3)

$$g_1 = \int_{\Omega} d\Omega - A_o \le 0, \qquad g_2 = \int_{\Omega_e} (\sigma_o^2/\sigma_a^2 - 1) \, d\Omega \le 0$$

where the undeformed contours Γ_2 and Γ_4 are treated as the design variables, and constraints g_1 and g_2 are identical to those specified previously.

B. State Equations of Thermoelastic Solids

The thermal deformation $u(x)$ according to the linear, quasistatic thermoelastic theory is the solution of the following equation of equilibrium:

$$\sigma_{ij,j} = 0 \qquad \text{in} \quad \Omega \tag{5}$$

with the stress-strain relationship

$$\sigma_{ij} = D_{ijkl}\epsilon_{kl}(u) - rT\delta_{ij} \qquad \text{in} \quad \Omega \tag{6}$$

or, in terms of matrix notations

$$\sigma = D\epsilon(u) - CT \tag{7}$$

where $\sigma = [\sigma_{ij}]$ and $\epsilon = [\epsilon_{ij}]$ are stress and strain tensors, respectively, and $D = [D_{ijkl}]$ and $C = [r\delta_{ij}]$ are matrices of material constants. Under the assumption of small strain, the linear strain-displacement relation can be applied to rewrite Eq. (7) in terms of displacements as

$$\sigma_{ij} = \lambda u_{k,k}\delta_{ij} = \nu(u_{i,j} + u_{j,i}) - rT\delta_{ij} \tag{8}$$

or in matrix form

$$\sigma = \lambda \nabla \cdot \boldsymbol{u} \cdot \boldsymbol{I} + \nu\left(\nabla \boldsymbol{u} + (\nabla \boldsymbol{u})^T\right) - rT \cdot \boldsymbol{I} \qquad \text{for } x \in \Omega \tag{9}$$

where $r = \alpha(2\nu + 3\lambda)$.

The temperature in the thermal stress problem, Eq. (6), can be obtained by solving the heat-transfer problem:

$$-k\nabla^2 T = 0 \qquad \text{in} \quad \Omega \tag{10}$$

For Eqs. (5) and (10) to warrant a unique solution, proper boundary conditions should be specified. With regard to the thermal fin problem as shown in Fig. 1, the linear thermoelasticity equation has the displacement u and traction t prescribed along Γ_1 and Γ_2 as

$$u = 0 \qquad \text{on} \ \Gamma_1 \tag{11a}$$

$$t = 0 \qquad \text{on} \ \Gamma_2 \tag{11b}$$

whereas the heat-transfer equation has the temperature and the heat-convection conditions imposed along Γ_1 and Γ_2, respectively, as

$$T = T_o \qquad \text{on} \ \Gamma_1 \tag{12a}$$

$$k\frac{\partial T}{\partial n} + h(T - T_\infty) = 0 \qquad \text{on} \ \Gamma_2 \tag{12b}$$

As for the fixed-fixed beam problem, a different set of boundary conditions is derived. The linear thermoelasticity equation entertains the following boundary conditions:

$$t = t^o \qquad \text{on} \ \Gamma_3 \tag{13a}$$

$$t = 0 \qquad \text{on} \ \Gamma_4 \tag{13b}$$

$$u = 0 \qquad \text{on} \ \Gamma_5 \tag{13c}$$

where the boundary contours Γ_3, Γ_4, and Γ_5 are defined in Fig. 2 and the only nonzero component, the y component, in the prescribed surface traction t^o is equal to the distributed load P_0. On the other hand, the heat-transfer equation is subjected to the following boundary conditions:

$$T = T_o \qquad \text{on} \ \Gamma_3 \tag{14a}$$

$$k\frac{\partial T}{\partial n} + h(T - T_\infty) = 0 \qquad \text{on} \ \Gamma_4 \tag{14b}$$

$$k\frac{\partial T}{\partial n} = 0 \qquad \text{on} \ \Gamma_5 \tag{14c}$$

where Eq. (14c) denotes the thermal insulation condition on Γ_5.

III. Shape Design Sensitivity Analysis of Linear, Quasistatic Thermoelastic Solids

Shape-design sensitivity analysis is used to calculate the design derivatives of system responses with respect to changes of shapes. With intensive research and development efforts, shape-design sensitivity analysis has been recently put into practical use in industry. Various approaches are reported in the literature to find shape-design sensitivities. Among them, the method of material derivatives is a popular choice. It has been employed[15,16] to perform shape-design sensitivity analysis of thermoelastic solids. These works describe a set of sensitivity equations that are boundary integrals defined along the boundary contours of thermoelastic solids. Because of its popularity, the method of material derivatives will also be employed in this study. However, in order to cope up with the numerical difficulties associated with the finite element method,[17] a different set of sensitivity equations that mainly consist of domain integrals is used.

In Sec. III.A, the method of material derivatives is briefly outlined. Section III.B introduces a direct-differentiation method to find the material derivatives $\dot{u}$ and $\dot{T}$. Section III.C employs the adjoint-variable method to derive the shape sensitivities of some generic functionals. Both methods in Secs. III.B and III.C are derived based upon the variational forms of state equations of a thermoelastic solid.

A. Method of Material Derivatives

Let the undeformed domain Ω be perturbed to a new configuration Ω^* due to a design modification. This perturbation can be viewed as a continuous transformation phenomenon between the original configuration Ω and the new one Ω^*. Let

point P occupy the coordinate x in Ω, and the new position of this point x^* in Ω^* is defined as

$$x^*(x,\tau) = x + \tau v(x) \tag{15}$$

where τ is a monitoring parameter and v is the position perturbation, denoted as the velocity field. Note that only the first-order term with respect to τ has been considered in the preceding representation in which $v(x)$ can be any vector function.

In the context of material derivatives, any function or functional should explicitly include the parameter τ as one of the independent variables to emphasize the direct relation between the function or functional and the varied domain. Hence, in shape-sensitivity analysis, a state variable $z(x)$ is usually defined as $z(x, 0)$ at $\tau = 0$ in the unperturbed domain and as $z(x^*, \tau)$ in the perturbed domain. The shape sensitivity of a function or functional can be mathematically represented by a derivative with respect to the time parameter "τ" appearing in Eq. (15). More specifically, the material derivative of a function $z(x)$ is defined as

$$\begin{aligned}\dot{z}(x) &= \dot{z}(x, 0) \\ &= \frac{dz}{d\tau}\Big|_{\tau=0} \\ &= \lim_{\tau\to 0}\frac{z(x+\tau v(x), \tau) - z(x, 0)}{\tau}\end{aligned} \tag{16}$$

With the preceding definition, the following relations can be easily proven,[4] and will be used later in the derivation

$$\dot{\overline{\nabla u}} = \nabla\dot{u} - \nabla v \cdot \nabla u \tag{17}$$

where the symbol $\dot{\overline{\square}}$ is defined as $d\square/d\tau|_{\tau=0}$ for any variable $\square$, and

$$\nabla v \cdot \nabla u = \sum_{j=1}^{3}\frac{\partial u_l}{\partial x_j}\frac{\partial v_j}{\partial x_k}: \quad l, k = 1, 2, 3 \tag{18}$$

The total material derivative of the strain tensor $\epsilon(u) = [\epsilon_{ij}(u)]$ can be obtained by

$$\begin{aligned}\dot{\overline{\epsilon(u)}} &= \dot{\overline{[\epsilon_{ij}(u)]}} = \tfrac{1}{2}\dot{\overline{[\nabla u + (\nabla u)^T]}} \\ &= \left[\epsilon(\dot{u}) - \tfrac{1}{2}[\nabla v \cdot \nabla u + (\nabla v \cdot \nabla u)^T]\right]\end{aligned} \tag{19}$$

Furthermore, with the definition of matrices $D = [D_{ijkl}]$ and $C = [C_{ij}]$, the material derivative of the stress tensor, $\sigma(u) = [\sigma_{ij}(u)]$, can be written as

$$\begin{aligned}\dot{\overline{\sigma(u)}} &= \dot{\overline{[\sigma_{ij}(u)]}} = [D_{ijkl}]\,\dot{\overline{[\epsilon_{kl}(u)]}} - [C_{ij}]\dot{T} \\ &= D\epsilon(\dot{u}) - \tfrac{1}{2}D\left[\nabla v \cdot \nabla u + (\nabla v \cdot \nabla u)^T\right] - C\dot{T}\end{aligned} \tag{20}$$

Next, defining general domain and boundary functionals in terms of temperature, thermal displacement, and stress as

$$J(\Omega) = \int_\Omega F[T, u, \sigma(u)]\, d\Omega \tag{21}$$

$$I(\Gamma) = \int_\Gamma G(T, t, u)\, ds \tag{22}$$

Their respective material derivatives can be obtained as

$$\dot{J}(\Omega) = \int_\Omega\left(\frac{\partial F}{\partial T}\dot{T} + \frac{\partial F}{\partial u}\dot{u} + \frac{\partial F}{\partial \sigma}\dot{\overline{\sigma(u)}} + F\,\mathrm{div}\,v\right) d\Omega \tag{23}$$

$$\dot{I}(\Gamma) = \int_\Gamma\left(\frac{\partial G}{\partial T}\dot{T} + \frac{\partial G}{\partial t}\dot{t} + \frac{\partial G}{\partial u}\dot{u}\right) ds + \int_\Gamma G\,\dot{\overline{ds}} \tag{24}$$

The computation of the second boundary integral in Eq. (24) can be represented[4] as

$$\int_\Gamma G\,\dot{\overline{ds}} = \int_\Gamma G[\nabla \cdot v - (\nabla v \cdot n)\cdot n]\, ds \tag{25}$$

where $\dot{\overline{ds}}$ denotes the material derivative of a differential arc length. An alternative formula is proposed hereafter to compute the preceding material derivative. It is noted that the boundary Γ is usually composed of piecewise straight segments, as a result of finite element discretization. Thus, the boundary integrals $I(\Gamma)$ and $\int_\Gamma G\,\dot{\overline{ds}}$, can be represented as

$$I(\Gamma) = \int_\Gamma G\, ds = \sum_{i=1}^{m}\int_o^{l_i} G\, ds \tag{26}$$

and

$$\int_\Gamma G\,\dot{\overline{ds}} = \sum_{i=1}^{m}\frac{\dot{l}_i}{l_i}\int_o^{l_i} G\, ds \tag{27}$$

where m is the number of linear segments, each with length l_i. The variation of a linear segment $\dot{l}_i$ can be expressed as a linear function of nodal velocities defined at the ends of the segment. Equation (27) will be implemented numerically to aid the shape-sensitivity calculations.

Finally, with all of the necessary relations being defined, one can proceed to derive sensitivity equations to compute $\dot{u}_i(x)$, $\dot{T}(x)$, $\dot{J}(\Omega)$, and $\dot{I}(\Gamma)$ of a thermoelastic solid.

B. Direct-Differentiation Method for Shape-Sensitivity Analysis of Thermoelastic Solids

To simplify the discussion, the derivation given in this section is pertaining to the thermal fin problem. However, with a simple modification, the conclusion can be directly extended to the fixed-fixed beam problem.

Let $\pi_\sigma = 0$ and $\pi_T = 0$ be the variational integrals associated with the state equations (5) and (10), respectively. Their detailed expressions are given as

$$\begin{aligned}\pi_\sigma &= \int_\Omega \sigma_{ij,j}\cdot p_i\, d\Omega = 0 \\ &= \int_\Omega \sigma\epsilon(p)\, d\Omega - \int_{\Gamma_1} t\cdot p\, ds\end{aligned} \tag{28}$$

$$\begin{aligned}\pi_T &= \int_\Omega -k\nabla^2 T\cdot g\, d\Omega = 0 \\ &= \int_\Omega k\nabla T\cdot\nabla g\, d\Omega - \int_{\Gamma_1} qg\, ds + \int_{\Gamma_2} h(T - T_\infty)g\, ds\end{aligned} \tag{29}$$

Note that the boundary conditions of the thermal fin problem, expressed by Eqs. (11) and (12), have been taken into account in the preceding formulation where p and g are arbitrary functions.

With the aid of Eqs. (15-17), the material derivatives of Eqs. (28) and (29) give

$$\begin{aligned}0 = \dot{\pi}_\sigma &= \int_\Omega\left[D\epsilon(\dot{u})\epsilon(p) - C\dot{T}\epsilon(p)\right] d\Omega \\ &- \int_{\Gamma_1}\dot{t}\cdot p\, ds + R\sigma(v, p)\end{aligned} \tag{30}$$

$$\begin{aligned}0 = \dot{\pi}_T &= \int_\Omega k\nabla\dot{T}\cdot\nabla g\, ds + \int_{\Gamma_1}\dot{q}g\, ds \\ &+ \int_{\Gamma_2} h\dot{T}g\, ds + R_T(v, g)\end{aligned} \tag{31}$$

where the remaining terms R_σ and R_T can be found as

$$R_\sigma(v, p) = -\int_\Omega \tfrac{1}{2}\sigma(u)(\nabla v \cdot \nabla p) + (\nabla v \cdot \nabla p)^T \, d\Omega$$
$$- \int_\Omega \tfrac{1}{2} D \nabla v \cdot \nabla u + (\nabla v \cdot \nabla u)^T \epsilon(p) \, d\Omega$$
$$+ \int_\Omega \sigma(u)\epsilon(p) \operatorname{div} v \, d\Omega - \int_{\Gamma_1} t \cdot p \, \dot{\overline{ds}} \tag{32}$$

$$R_T(v, g) = -\int_\Omega \tfrac{1}{2} k[(\nabla v \cdot \nabla T) \cdot \nabla g$$
$$+ \nabla T \cdot (\nabla v \cdot \nabla g)] \, d\Omega + \int_\Omega k \nabla T \cdot \nabla g \operatorname{div} v \, d\Omega$$
$$+ \int_{\Gamma_2} h(T - T_\infty) g \, \dot{\overline{ds}} \tag{33}$$

Careful examination reveals that the integrals presented in Eqs. (30) and (31) are indeed variational integrals for $\dot{u}$ and $\dot{T}$ in which the $R_\sigma(v, p)$ term may be viewed as the virtual work done by a body force and the $R_T(v, g)$ term may be considered as the energy term generated by a distributed heat source. Moreover, by taking material derivatives of the boundary conditions of the original state equations, Eqs. (11) and (12), one obtains the proper boundary conditions required for uniquely solving Eqs. (30) and (31):

$$\dot{u} = 0 \quad \text{on} \quad \Gamma_1 \tag{34a}$$

$$\dot{t} = 0 \quad \text{on} \quad \Gamma_2 \tag{34b}$$

$$\dot{T} = 0 \quad \text{on} \quad \Gamma_1 \tag{35a}$$

$$\dot{q} + h\dot{T} = 0 \quad \text{on} \quad \Gamma_2 \tag{35b}$$

The preceding boundary conditions help to specify the Euler-Lagrange equations of Eqs. (30) and (31) as

$$\sigma_{ij,j} = B_i \tag{36}$$

and

$$-k \nabla^2 \dot{T} = Q \tag{37}$$

where the stress-strain relation is described by

$$\sigma_{ij} = D_{ijkl} \epsilon_{kl}(\dot{u}) - r\dot{T}\delta_{ij} \tag{38}$$

and the body force B_i and the internal heat source Q are generated by the terms $R_\sigma(\dot{v}, p)$ and $R_T(v, g)$, respectively. In view of the original equations for u and T, the material derivatives $\dot{u}$ and $\dot{T}$ may be viewed as the pseudodisplacement and the pseudotemperature defined in a linear quasistatic thermoelastic solid. This thermoelastic solid is subjected to a body force and an internal heat source with zero T_o and T_∞ prescribed on Γ_1 and Γ_2, respectively. Consequently, the same finite-element matrix equation used for solving u and T can be applied here again, with a different force vector to solve for $\dot{u}$ and $\dot{T}$. Hence, one can take the advantage of the fact that the stiffness matrix has already been triangularized to reduce computational effort in solving $\dot{u}$ and $\dot{T}$.

Note that $\dot{u}$ and $\dot{T}$ are linearly dependent upon the position perturbation $v(x)$ as indicated in the right-hand side terms of Eqs. (30) and (31). In other words, substituting basic vector $cv_i(x)$ for $v(x)$ into R_σ and R_T, we have $c\dot{u}_i(x)$ and $c\dot{T}_i(x)$ as solutions for an arbitrary constant c. Consequently, $\dot{u}(x) = \sum b_i \dot{u}_i(x)$ are the shape derivatives of $u(x)$ with respect to the design velocity $v(x)$ which is equal to $\sum b_i v_i(x)$, a linear combination of basic vectors $v_i(x)$.

In the following examples, the basic vectors $v_i(x)$ for $x \epsilon \Omega$ are constructed by analyzing a two-dimensional elastic problem defined in $\Omega \cup \Gamma$ with a unit load applied at each of the nodes along the varied boundary. This elastic problem will be solved by the finite element method. Each of such loads, called the fictitious load, will generate a displacement field that will be defined as a basic vector v_i. As shown in Fig. 1, the velocity field of the thermal fin has eight basic vectors, each of which is the displacement caused by a unit load indicated by an integer. The weighting factor of each basic vector b_i will be considered as a design variable. Thus, there are eight design variables in the shape optimization of the thermal fin.

The validity of the solution procedure discussed here is examined by numerically calculating $\dot{T}$ and $\dot{u}$ for the thermal fin problem. The finite element model shown in Fig. 1 will be used for the heat-transfer analysis, Eq. (10), as well as the thermal stress analysis, Eq. (5). Note that $\dot{T}$ has to be solved first before $\dot{u}$ can be solved by using Eq. (30).

The geometric dimension of the thermal fin is as follows: the height of the fin is, from the tip to the base, 10 units and the width of the base is 10 units as well. The numerical results evaluated for the thermal fin problem, tabulated in Table 1, are obtained based upon the following nondimensional properties: $E = 0.2067 \times 10^5$, $\nu = 0.334$, $\alpha = 0.12 \times 0^{-3}$, $h = 0.005$, $k = 1.0$, $T_o = 500$, and $T_\infty = 300$. The values in the second and fourth columns denote the exact difference between the unperturbed and the perturbed horizontal displacement and temperature at the point where the fictitious load is applied. On the other hand, the values in the third and fifth columns are calculated by using the approximations $\Delta u_x = \dot{u}_x \cdot \Delta b_i$ and $\Delta T = \dot{T} \cdot \Delta b_i$. The change in design variables Δb_i is equal to 1 in this example. The numerical results show that the $\dot{u}$ and $\dot{T}$ are computed with high precision.

C. Adjoint-Variable Method for Shape-Sensitivity Analysis of Thermoelastic Solids

The adjoint-variable method will be employed in this section to derive shape sensitivities of functionals defined in the shape-optimization problems discussed earlier. For simplicity, a generic functional ψ will be adopted here to illustrate the derivation procedure:

$$\psi = \int_\Omega f(T,\sigma) \, d\Omega + \int_{\Gamma_a} \beta(q) \, ds + \int_{\Gamma_b} \lambda(u) \, ds \tag{39}$$

In the preceding functional, $f(T,\sigma)$, $\beta(q)$, and $\lambda(u)$ are defined as a function of the temperature and stress over the domain Ω, the heat flux on the boundary region Γ_a, and the displacement distribution on the boundary region Γ_b, respectively. Let the generic functional be defined in a thermoelastic solid subjected to external loadings and thermal effects with the following natural boundary conditions:

$$t = t^o \quad \text{on} \quad \Gamma_a \tag{40a}$$

$$t = 0 \quad \text{on} \quad \Gamma_b \tag{40b}$$

$$q = 0 \quad \text{on} \quad \Gamma_c \tag{40c}$$

The variational equalities of π_σ and π_T associated with this problem can be written as

$$\pi_\sigma = 0$$
$$= \int_\Omega \sigma\epsilon(p) \, d\Omega - \int_{\Gamma_a} t^o \cdot p \, ds - \int_{\Gamma_c} t \cdot p \, ds \tag{41}$$

$$\pi_T = 0$$
$$= \int_\Omega k \nabla T \cdot \nabla g \, d\Omega + \int_{\Gamma_b} h(T - T_\infty) g \, ds - \int_{\Gamma_a} qg \, ds \tag{42}$$

Table 1 Shape-sensitivity coefficients by using direct-differentiation method

Design variables, b_i	Changes in u_x, 10×10^{-6}	First-order approximation, 10×10^{-6}	Changes in T, 10×10^{-4}	First-order approximation, 10×10^{-4}
1	1.626508	1.626533	− 2.240880	− 2.240876
2	2.959593	2.959780	− 3.883854	− 3.883847
3	2.909182	2.909589	− 5.014175	− 5.014163
4	1.734405	1.735036	− 5.649520	− 5.648506
5	− 0.140420	− 0.139587	− 5.677201	− 5.677189
6	− 2.455845	− 2.454830	− 4.835271	− 4.835258
7	− 5.239494	− 5.238366	− 2.546009	− 2.545953
8	− 8.056798	− 8.055815	2.723496	2.723858

where the heat-convection condition is imposed on Γ_b. Nevertheless, the above equations help to redefine the functional ψ as $\psi = \psi + \pi_\sigma + \pi_T$ whose material derivative is then given as $\dot{\psi} = \dot{\psi} + \dot{\pi}_\sigma + \pi_T$. The first term on the right-hand side can be derived by using Eqs. (15–27) as

$$\dot{\psi} = \int_\Omega \left(\frac{\partial f}{\partial T}\dot{T} + \frac{\partial f}{\partial \sigma}\dot{\sigma}\right) d\Omega + \int_\Omega f \operatorname{div} v \, d\Omega + \int_{\Gamma_a}\left(\frac{\partial \beta}{\partial q}\right)\dot{q}\, ds + \int_{\Gamma_b}\left(\frac{\partial \gamma}{\partial u}\right)\cdot \dot{u}\, ds + \int_{\Gamma_a}\beta \dot{\overline{ds}} + \int_{\Gamma_b}\gamma \dot{\overline{ds}}$$
$$= \int_\Omega \left(\frac{\partial f}{\partial T}\dot{T} + \frac{\partial f}{\partial \sigma}D\epsilon(\dot{u}) - \frac{\partial f}{\partial \sigma}C\dot{T}\right) d\Omega + \int_{\Gamma_a}\left(\frac{\partial \beta}{\partial q}\right)\dot{q}\, ds + \int_{\Gamma_b}\left(\frac{\partial \gamma}{\partial u}\right)\cdot \dot{u}\, ds + R_\psi(v,u) \tag{43}$$

where the remainder term $R_\psi(v, u)$ can be found as

$$R_\psi(v, u) = -\frac{1}{2}\int_\Omega \frac{\partial f}{\partial \sigma} D[\nabla v \cdot \nabla u + (\nabla v \cdot \nabla u)^T]\, d\Omega + \int_\Omega f \operatorname{div} u \, d\Omega + \int_{\Gamma_a}\beta \dot{\overline{ds}} + \int_{\Gamma_b}\gamma \dot{\overline{ds}} \tag{44}$$

Similarly, $\dot{\pi}_\sigma = 0$ and $\dot{\pi}_T = 0$ yield

$$0 = \dot{\pi}_\sigma = \int_\Omega [D\epsilon(\dot{u})\epsilon(p) - C\dot{T}\epsilon(p)]\, d\Omega - \int_{\Gamma_c}\dot{t}\cdot p\, ds + R_\sigma(v, p) \tag{45}$$

$$0 = \dot{\pi}_T = \int_\Omega (k\nabla \dot{T}\cdot \nabla g)\, d\Omega - \int_{\Gamma_a}\dot{q}g\, ds + \int_{\Gamma_b} h\dot{T} g\, ds + R_T(v, g) \tag{46}$$

where $R_\sigma(v, p)$ and $R_T(v, g)$ are summarized as

$$R_\sigma(v, p) = -\int_\Omega \frac{1}{2}\sigma(u)\cdot[(\nabla v \cdot \nabla p) + (\nabla v \cdot \nabla p)^T]\, d\Omega - \int_\Omega \frac{1}{2} D[\nabla v \cdot \nabla u + (\nabla v \cdot \nabla u)^T]\epsilon(p)\, d\Omega + \int_\Omega \sigma(u)\epsilon(p) \operatorname{div} v \, d\Omega - \int_{\Gamma_a} t^o \cdot p \, \dot{\overline{ds}} \tag{47}$$

$$R_T(v, g) = -\int_\Omega k[(\nabla v \cdot \nabla T)\cdot \nabla g + \nabla T \cdot (\nabla v \cdot \nabla g)^T]\, d\Omega + \int_\Omega k\nabla T \cdot \nabla g \operatorname{div} v \, d\Omega + \int_{\Gamma_b} h(T - T_\infty) g \, \dot{\overline{ds}} \tag{48}$$

Note that the preceding derivation is based on the following relations:

$$\dot{t}^o = 0 \qquad \text{on} \quad \Gamma_a \tag{49a}$$

$$\dot{t} = 0 \qquad \text{on} \quad \Gamma_b \tag{49b}$$

$$\dot{q} = 0 \qquad \text{on} \quad \Gamma_c \tag{49c}$$

and the assumption that the boundary Γ_c is not varied, which results in $\dot{\overline{ds}} = 0$ on Γ_c. Rearranging Eqs. (45–48) yields

$$\dot{\psi} = \left[\int_\Omega D\left(\epsilon(p) + \frac{\partial f}{\partial \sigma}\right)\epsilon(\dot{u})\, d\Omega + \int_{\Gamma_b}\left(\frac{\partial \gamma}{\partial u}\right)\cdot \dot{u}\, ds - \int_{\Gamma_c}\dot{t}\cdot p\, ds\right] + \left[\int_\Omega \left(k\nabla g \cdot \nabla \dot{T} + \left[\frac{\partial f}{\partial \sigma} - C\epsilon(p) - \frac{\partial f}{\partial \sigma}C\right]\dot{T}\right) d\Omega + \int_{\Gamma_a}\left(\frac{\partial \beta}{\partial q} + g\right)\dot{q}\, ds + \int_{\Gamma_b} h\dot{T} g\, ds\right] + R\psi(v, u) + R_\sigma(v, p) + R_T(v, g) \tag{50}$$

for arbitrary functions $p(x)$ and $g(x)$. One may specify these two arbitrary functions such that all terms involving $\dot{u}$ and $\dot{T}$ become zero and can then be eliminated from $\dot{\psi}$. For example, define the adjoint variable λ such that λ is the solution of the following adjoint equation for any arbitrary z:

$$\int_\Omega D\left[\epsilon(\lambda) + \frac{\partial f}{\partial \sigma}\right]\epsilon(z)\, d\Omega + \int_{\Gamma_b}\left(\frac{\partial \gamma}{\partial u}\right) z\, ds - \int_{\Gamma_c} t(z)\lambda\, ds = 0 \tag{51}$$

If the arbitrary function p is replaced by the adjoint variable λ, the terms in the first bracket of Eq. (50) will become zero because of Eq. (51), regardless of the values of $\dot{u}$. The adjoint equation, Eq. (51), can be viewed as a variational identity for the adjoint structure with the displacement field λ, which satisfies

$$\sigma_{ij,j} = 0 \qquad \text{in} \quad \Omega \tag{52}$$

and boundary conditions

$$t(\lambda) = 0 \qquad \text{on} \quad \Gamma_a$$
$$t(\lambda) = -\frac{\partial \gamma}{\partial u} \qquad \text{on} \quad \Gamma_b \tag{53}$$
$$\lambda = 0 \qquad \text{on} \quad \Gamma_c$$

where the constitutive equation is given as

$$\sigma_{ij}(\lambda) = D_{ijkl}\epsilon_{kl}(\lambda) + D_{ijkl}\frac{\partial f}{\partial \sigma_{kl}} \tag{54}$$

The last term in the constitutive relation can be considered as an initial stress appearing in the adjoint structure. Similarly, one can define another adjoint variable $\mu(x)$ to be the solution

of the following identity for any arbitrary function $w(x)$:

$$0 = \int_\Omega \left[k \nabla\mu \cdot \nabla w - \left(\frac{\partial f}{\partial T} + C\epsilon(\lambda) - \frac{\partial f}{\partial \sigma} C \right) w \right] d\Omega + \int_{\Gamma_a} -k \left(\frac{\partial \beta}{\partial q} + \mu \right) \dot{q}(w)\, ds + \int_{\Gamma_b} hw\mu\, ds = \int_\Omega \left[-k \nabla^2 \mu - \frac{\partial f}{\partial T} - C\epsilon(\lambda) + \frac{\partial f}{\partial \sigma} C \right] w\, d\Omega + \int_{\Gamma_a} -k \left[\left(\frac{\partial \beta}{\partial q} + \mu \right) \dot{q}(w) \right] ds + \int_{\Gamma_b} \left(k \frac{\partial \mu}{\partial n} + h\mu \right) w\, ds + \int_{\Gamma_c} k \frac{\partial \mu}{\partial n} w\, ds \tag{55}$$

and the following differential equations can be used to determine μ

$$\begin{aligned} k \nabla^2 \mu &= -\frac{\partial f}{\partial T} - C\epsilon(\lambda) + \frac{\partial f}{\partial \sigma} C \qquad \text{in} \quad \Omega \\ \frac{\partial \beta}{\partial q} + \mu &= 0 \qquad \text{on} \quad \Gamma_a \\ k \frac{\partial \mu}{\partial n} + h\mu &= 0 \qquad \text{on} \quad \Gamma_b \\ k \frac{\partial \mu}{\partial n} &= 0 \qquad \text{on} \quad \Gamma_c \end{aligned} \tag{56}$$

where the term $(\partial f/\partial T) - C\epsilon(\lambda) - (\partial f/\partial \sigma)C$ may be considered as the distributed heat source generated by the strain field $\epsilon(\lambda)$ of the adjoint structure defined in Eq. (51). Note that substituting μ for g and w for $\dot{T}$ into Eq. (50) makes the second bracketed term of Eq. (50) become zero with the condition $\dot{T} = 0$ on Γ_a. Finally, one obtains a simpler form of $\dot{\psi}$ by replacing the arbitrary variables in Eq. (50) by the adjoint variables

$$\dot{\psi} = R_\psi(v, u) + R_\sigma(v, \lambda) + R_T(v, \mu) \tag{57}$$

where $\dot{\psi}$ is clearly a linear functional of the design velocity $v(x)$.

It is interesting to note that the adjoint structure, described by Eqs. (52–54), can no longer be considered as a thermoelastic solid. In fact, the adjoint "temperature" can be solved only after the adjoint "displacement" has been first solved. This solution procedure reverses the sequence of solving a linear, quasistatic thermoelastic solid. Nevertheless, the finite element matrix equations established for solving the original system of Eqs. (5) and (10) can be directly applied here, with a modification of the force vectors, to evaluate the adjoint variables.

The adjoint equations, Eqs. (52–54) and (56), are derived from the generic functional of Eq. (39). Hence, in order to address the specified application problems studied in this paper, these adjoint equations need to be modified.

For the thermal fin problem, the boundary conditions of the generic problem should be modified as follows: Γ_a is Γ_1; Γ_b is Γ_2; and Γ_c is discarded in this case. The objective function given in Eq. (1) provides $f = \gamma = 0$ and $\partial\beta/\partial q = 1$. Furthermore, in view of the stress constraint given in Eq. (3), one can specify $\partial f/\partial T = \beta = \gamma = 0$ and $\partial f/\partial \sigma = 0$ everywhere except in the element of concern, Ω_e. As for the fixed-fixed beam problem, the boundary segments of the generic problem are redefined as follows: Γ_a is Γ_3; Γ_b is Γ_4; and Γ_c is Γ_5. Furthermore, the objective function of this fixed-fixed beam problem can be represented by the generic functional with the following modifications: $f = \beta = 0$ and $\partial\gamma/\partial w = 2(y + w - y_o)$.

Next, the finite element models of the thermal fin and the fixed-fixed beam are shown in Figs. 1 and 2 with 162 and 120 constant-strain-triangle elements, respectively.

In this study, the thermal fin problem has eight design variables and the fixed-fixed beam problem has 20 design variables. Note that symmetry has been considered in constructing Fig. 2b. The geometric dimension, material properties, and thermal loading of the thermal fin problem are the same as those given in Sec. III.B. For the fixed-fixed beam problem, the geometric dimension is a 20 units by 3 units rectangular beam subjected to a uniform loading of $P_0 = 100$ units with the following nondimensional properties: $E = 1 \times 10^5$, $\nu = 0.25$, $\alpha = 0.12 \times 10^{-4}$, $h = 0.005$, $k = 1.0$, $T_o = 80$, and $T_\infty = -100$. With the aid of the finite-element method, thermal stress analysis, basic velocity calculation, and adjoint-variable analysis can be accomplished by using the same finite-element model. The shape-sensitivity integrals of Eq. (57) can then be evaluated numerically. The validity of Eq. (57) is verified by comparing the actual changes in functionals due to small design perturbations to the changes approximated by using the first-order Taylor's series expansion. Note that in this numerical study, every design variable is perturbed by the same amount of variation.

The numerical results reported in Figs. 3–5 clearly validate the sensitivity equations presented in this section.

IV. Shape Optimization of Thermoelastic Solids

Once thermal stresses, displacements, and design-sensitivity coefficients are calculated, one can proceed to perform shape optimization. The gradient-based, optimization algorithm selected in this study is called LINRM, a recursive quadratic programming algorithm with an active set strategy. The detailed derivation of this algorithm can be found in Refs. 18 and 19. The fundamental concept of this algorithm is that, rather than directly solving the optimality criteria, a small perturbation for each design variable is determined in each iteration to reduce the objective function and correct the violations. In this algorithm, the changes in the objective function and the constraint violations are approximately represented by the design-sensitivity coefficients. Furthermore, it has been proven that the LINRM can converge to a local minimum as soon as the l^2 norm of the perturbation of design variables approaches zero. Thus, the l^2 norm of the perturbation of

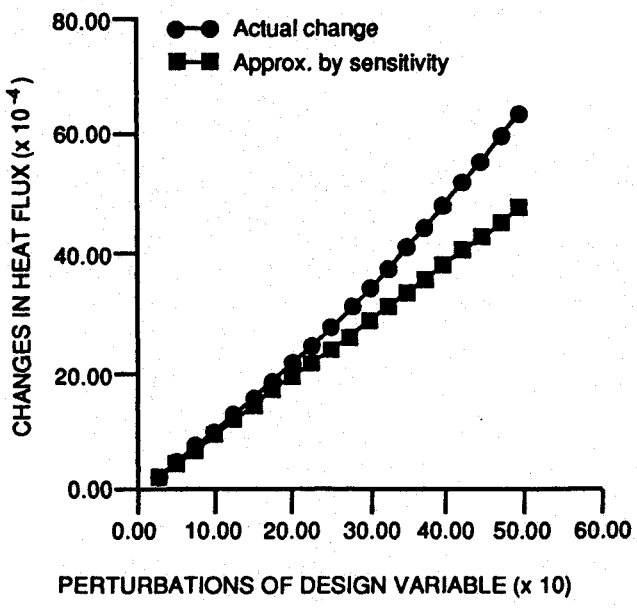

Fig. 3 Shape-sensitivity analysis of heat flux functional (thermal fin problem).

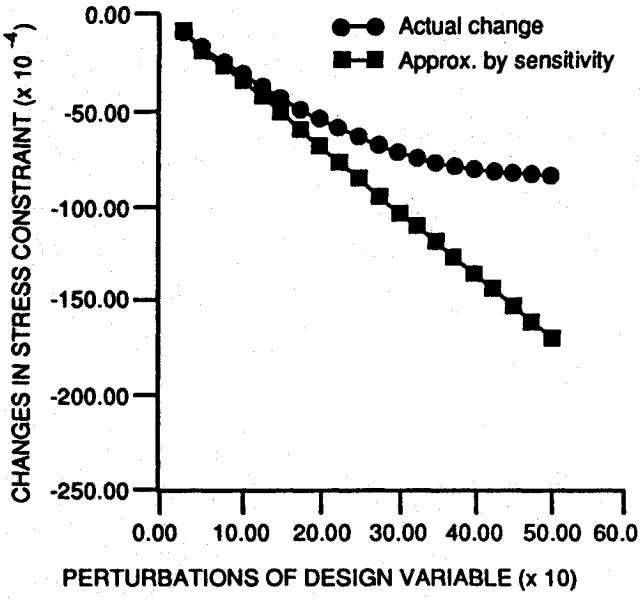

Fig. 4 Shape-sensitivity analysis of stress functional (thermal fin problem).

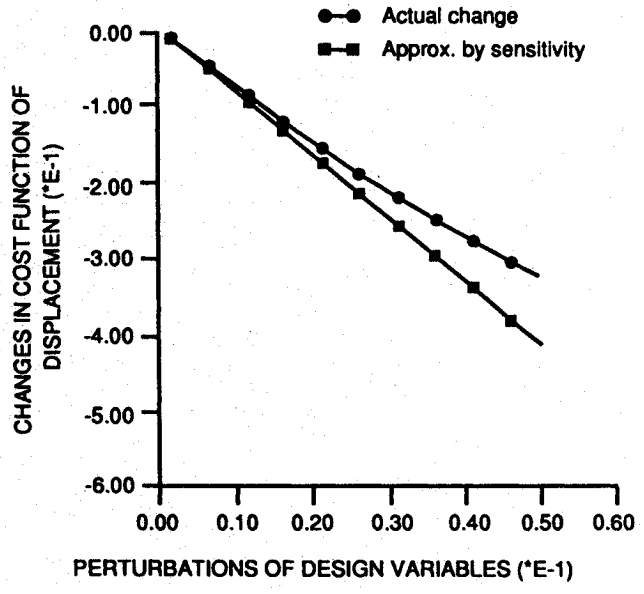

Fig. 5 Shape-sensitivity analysis of displacement functional (fixed-fixed beam).

design variables is often used as a convergence criterion in LINRM.

The conceptual procedure for shape optimization of a thermoelastic problem is outlined as follows:

1) Start with an initial geometry.

2) Function evaluation: a) Solve temperature distribution $T(x)$ from the heat-transfer problem, Eq. (10). b) Calculate the thermal deformation $u(x)$ from the state equation of a linear, quasistatic thermoelastic solid, Eq. (5).

3) Gradient evaluation: a) Construct basic vectors $v_i(x)$. b) Formulate the adjoint loading for the adjoint structure. c) Solve the adjoint displacement, Eqs. (52–54). d) Solve the adjoint temperature, Eq. (56). e) Calculate shape-sensitivity coefficients, Eq. (57).

4) Design improvement using LINRM algorithm: a) Solve a quadratic subproblem to find the best search direction. b) Use one-dimensional search to find a proper step size.

5) Update the configuration profile.

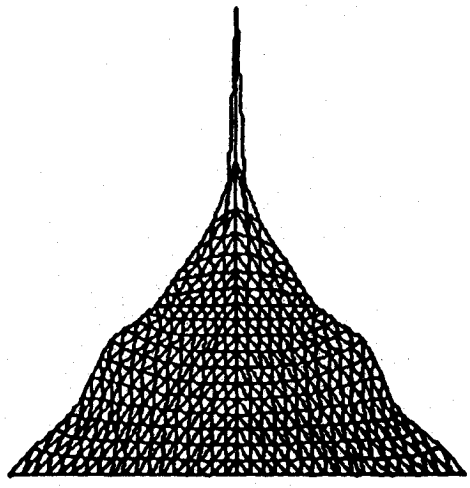

Fig. 6a Shape optimization of a thermal fin (case 1).

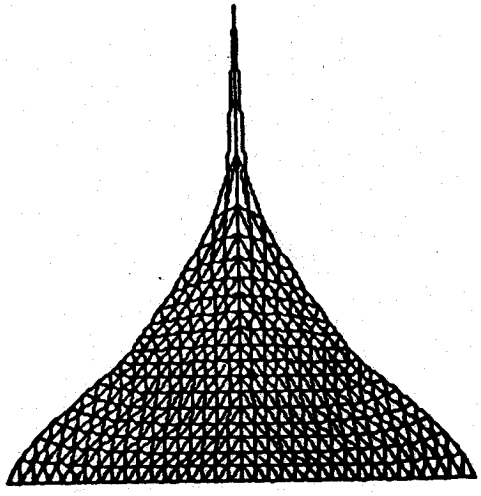

Fig. 6b Shape optimization of a thermal fin (case 2).

6) Check the convergence criteria. If the convergence criteria satisfy, stop. Otherwise, go back to step 1.

Two design problems, the thermal fin and the fixed-fixed beam, are to be investigated in the following sections.

A. Shape Optimization of a Thermal Fin

The design formulation for shape optimization of a thermal fin is described by Eqs. (1–3). The initial design of a thermal fin is a triangle with an area of 50 units. A finite element mesh finer than the one shown in Fig. 1 will be adopted in this study, consisting of 361 nodes and 648 constant-strain-triangle (CST) elements. The area is constrained not to exceed 30 units and the maximum allowable stress in the stress constraint is equal to 140 units. The information of geometric dimension and material properties have been given in the numerical example in Sec. III.B. There are 34 design variables assigned to describe the profile of Γ_2. The results may be summarized as follows:

Case 1

The objective function F_b defined by Eq. (1) is maximized to find the optimal profile of a thermal fin. The only constraint considered in this case is the area constraint, Eq. (2). It takes eight iterations of LINRM to reach convergence. The optimal profile is shown in Fig. 6a. The objective function changes from an initial design of 21.20 units to a final value of 20.92 units. At the final stage, the area becomes 30.0 units and the maximum Von Mises stress 212.73 units.

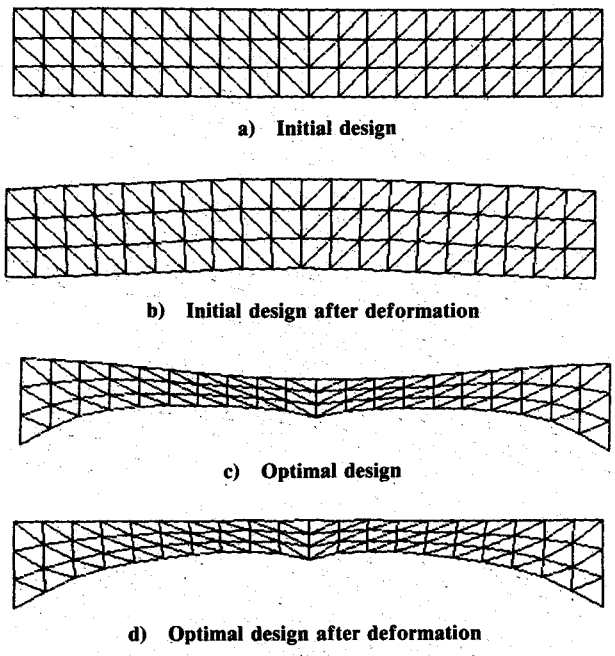

a) Initial design

b) Initial design after deformation

c) Optimal design

d) Optimal design after deformation

Fig. 7 Shape optimization of a loaded fixed-fixed beam.

Case 2

In this case, the stress constraint, Eq. (3), is included in the problem formulation. It takes nine iterations to arrive at the optimal solution in which the final objective function becomes 20.95 units. The optimal profile, shown in Fig. 6b, has an area of 30.0 units and the maximum Von Mises stress is 124.76 units. Note that the optimal design of this case is slightly better than that of the preceding one. A possible explanation is that the shape-optimization problem of a thermal fin has many local minima as reported in Refs. 20 and 21, which can easily trap the LINRM algorithm known to be quite sensitive to a local minimum.[18]

B. Shape Optimization of a Uniformly Loaded Beam

This example will determine the initial geometry of a loaded, fixed-fixed beam shown in Fig. 2, subject to an area and a stress constraint, such that the top edge of the deformed beam will stay straight. The objective function of the design problem is mathematically described by Eq. (4).

The finite element model of the beam consists of 84 nodes and 120 CST elements. The information of geometric dimension, material properties, and loadings are provided in the numerical example in Sec. III.C. The area is constrained not to exceed 30 units and the maximum allowable stress is given as 1467 units. The reference datum y_o is set to 3 units, and there are 20 design variables assigned to describe the boundaries Γ_3 and Γ_4, as shown in Fig. 2b. The optimization algorithm, LINRM, takes four iterations to reach the optimal solution. The geometrical configurations of the initial and the optimal beams, with and without deformation, are given in Fig. 7. The initial values of the objective, the area, and the stress constraints are 0.533, 60, and 1117 units, respectively, which are varied to 0.003, 30, and 1460 units, respectively, at the optimum design.

V. Discussion and Concluding Remarks

The main objective of this research was to develop a theoretical derivation and perform numerical studies for shape-sensitivity analysis and design optimization of thermoelastic solids, which have been demonstrated with great accuracy.

Using both the direct-differentiation and adjoint-variable techniques, the mathematical formulation for shape-sensitivity analysis of various domain and boundary integrals have been reported in Sec. III. The shape-sensitivity equations have been represented in the form of linear functionals of design velocity. The finite element method has been established to evaluate shape-sensitivity coefficients numerically. The results of the numerical study show that the computational scheme discussed in this section is a valid appproach. Furthermore, there are two observations worthwhile mentioning here:

1) The sensitivity equations derived by either the direct-differentiation or the adjoint-variable technique are very much similar to the state equations governing thermoelastic solids. Consequently, in the entire direct-equation solving procedure, calculation of the total variations $\dot{u}$ and $\dot{T}$ or the adjoint variables can be efficiently performed without matrix factorization.

2) The state equations of a linear, quasistatic thermoelastic solid are uncoupled for temperature and thermal displacement calculations. The computational procedure usually starts with heat-transfer analysis followed by thermal stress analysis. However, the adjoint equations, although in the same form as the state equations of thermoelasticity, yield a different physical interpretation and a different solution procedure. The adjoint structure is not a thermoelastic solid by an elastic one with initial stress, in which the "adjoint stress" has to be calculated first before the "adjoint temperature" can be found.

References

[1]Bennett, J. A., and Botkin, M. E. (eds.), *The Optimum Shape: Automated Structural Design,* Plenum, New York, 1986.

[2]Pironneau, O., *Optimal Shape Design for Elliptic Systems,* Springer-Verlag, New York, 1985.

[3]Mota Soares, C. A., (ed.), *Computer-Aided Optimal Design: Structural and Mechanical System,* Springer-Verlag, Berlin, Heidelberg, 1987.

[4]Haug, E. J., Choi, K. K., and Komkov, V., *Design Sensitivity Analysis of Structural Systems,* Academic, Orlando, FL, 1985, Chap. 3.

[5]Hafka, R. T., and Grandhi, R. V., "Structural Shape Optimization—A Survey," *Computer Methods in Applied Mechanics and Engineering,* Vol. 57, No. 1, 1986, pp. 91–106.

[6]Meric, R. A., "Shape Design Sensitivity Analysis for Nonlinear Anisotropic Heat-Conducting Solids and Shape Optimization by BEM," *International Journal for Numerical Methods in Engineering,* Vol. 26, No. 1, 1988, pp. 109–120.

[7]Dems, K., and Mroz, Z., "Variational Approach by Means of Adjoint Systems to Structural Optimization and Sensitivity Analysis. I: Variational of Material Parameters within Fixed Domain," *International Journal of Solids and Structures,* Vol. 19, No. 8, 1983, pp. 677–692.

[8]Dems, K., and Mroz, Z., "Variational Approach by Means of Adjoint Systems to Structural Optimization and Sensitivity Analysis. II: Structure Shape Variation," *International Journal of Solids and Structures,* Vol. 20, No. 6, 1984, pp. 527–552.

[9]Curtis, J. P., "Optimization of Homogeneous Thermal Insulation Layer," *International Journal of Solids and Structures,* Vol. 19, No. 9, 1983, pp. 831–823.

[10]Banichuk, N. V., "Optimization of Elastic Bars in Torsion," *International Journal of Solids and Structures,* Vol. 12, No. 4, 1976, pp. 275–286.

[11]Zienkiewicz, O. C., and Campbell, J. S., "Shape Optimization and Sequential Linear Programming," *Optimum Structural Design,* edited by R. H. Gallagher and O. C. Zienkiewicz, Wiley, New York, 1973, pp. 109–126.

[12]Gelfand, J. M., and Fomin, S. V., *Calculus of Variations,* Prentice-Hall, Englewood Cliffs, NJ, 1963, Chap. 3.

[13]Yang, R. J., and Botkin, M. E., "Accuracy of the Domain Material Derivative Approach to Shape-Design Sensitivities," *AIAA Journal,* Vol. 25, No. 12, 1987, pp. 1606–1610.

[14]Yang, R. J., and Botkin, M. E., "Comparison Between the Variational and Implicit Differentiation Approaches to Shape-Design Sensitivities," *AIAA Journal,* Vol. 24, No. 6, 1986, pp. 1027–1032.

[15]Dems, K., "Sensitivity Analysis in Thermoelastic Problems," *Computer-Aided Optimal Design: Structural and Mechanical Sys-*

tems, NATO ASI Series F, edited by C. A. Mota Soares, Springer-Verlag, New York, 1987, pp. 563–572.

[16]Meric, R. A., "Boundary Elements in Shape-Design Sensitivity Analysis of Thermoelastic Solids," *Computer-Aided Optimal Design: Structural and Mechanical Systems,* NATO ASI Series F, edited by C. A. Mota Soares, Springer-Verlag, New York, 1987, pp. 643–652.

[17]Hou, J. W., Chen, J. L., and Sheen, J. S., "Computational Method for Optimization of Structural Shapes," *AIAA Journal,* Vol. 24, No. 6, 1986, pp. 1005–1012.

[18]Choi, K. K., Huag, E. J., Hou, J. W., and Sohoni, V. N., "Pshenichny's Linearization Method for Mechanical System Optimization," *ASME Journal of Mechanisms, Transmissions, and Automation in Design,* Vol. 105, No. 1, 1983, pp. 97–103.

[19]Pshenichny, B. N., and Danilin, Y. M., *Numerical Methods in External Problems,* MIR Publishers, Moscow, 1978, Chap. 3, Sec. 5.

[20]Maday, C. J., "The Minimum Weight One-Dimensional Straight Cooling Fin," *ASME Journal of Engineering for Industry,* Vol. 96, No. 2, 1974, pp. 1161–1165.

[21]Sheen, J. S., "Computational Methods for Shape Optimization," Ph.D. Dissertation, Old Dominion Univ., Norfolk, VA, 1989.